13th Manufacturing Science and Engineering Conference
MSEC2018
June 18-22, 2018, College Station, TX

MSEC2018-6442

BUILDING BLOCK-BASED ASSEMBLY OF SCALABLE METALLIC LATTICES

Benjamin Jenett
Center for Bits and Atoms, MIT
Cambridge, MA, USA.
bej@mit.edu

Neil Gershenfeld
Center for Bits and Atoms, MIT
Cambridge, MA, USA.
neil.gershenfeld@cba.mit.edu

Paul Guerrier
Moog Inc.
East Aurora, NY, USA.
pguerrier@moog.com

ABSTRACT

We describe a method for the manufacturing of metallic lattices with tunable properties through the reversible assembly of building block elements, which we call discrete metal lattice assembly (DMLA). These structures can have sub-millimeter scale features on millimeter scale parts used to assemble structures spanning tens of centimeters, comparable to those currently made with Direct Metal Laser Sintering (DMLS). However, unlike traditional additive manufacturing (AM) methods, the use of discrete assembly affords a number of benefits, such as extensible, incremental construction and being repairable and reconfigurable. We show this method results in large scale (tens of centimeters), ultralight (<10 kg/m^3 effective density) lattices which are currently not possible with state of the art additive manufacturing techniques. The lattice geometry used here is a combination of two geometries with quadratic property scaling, resulting in a novel lattice with sub-quadratic scaling.

INTRODUCTION

Recently much interest has been shown in the use of lattice geometries to design novel meta-materials, which can be understood as interconnected networks of struts and nodes, with unique and desirable mechanical properties when considered as a bulk material. These structures get their properties from their base materials, their geometry, and their density [1]. They are also well suited for space and aviation applications due to high stiffness and strength to weight ratios.

While the analytical description of these structures, known as architected cellular solids, is well described [2], their manufacturing methods remain an open topic for research. Recently it has been shown that micro-stereolithography can be used to make micrometer scale features in photoreactive polymer, which can then be coated with metal, and the polymer removed to yield hollow metal micro lattice with ultralight density and novel stiffness properties [3]. This process, which we will refer to as "Additive Manufacturing and Deposition" (AMD) can be used to make hierarchical structures on the order of centimeters in scale [4] [5] [6], but faces challenges with larger scales, due to the machine scaling with the size of the specimen.

Other approaches for metallic lattices include interleaving sets of cut or folded sheet metal, which are then welded to boundary skins to form sandwich structures [7]. Open lattice structures can be formed through a combination of punching, folding, and laminating, with a final welding step [8].

Large scale metal components with complex geometries can be made with metal laser additive manufacturing (MLAM) in which a bed of metal powder is selectively melted with a laser to form a continuous metal component, layer by layer. This approach has gained attention for its ability to save weight and make complex geometry at minimal cost with applications in fields such as aerospace and robotics.

A recent approach to lattice manufacturing is based on the reversible assembly of modular, building block elements. This expands upon the existing work of cellular solids by decomposing the periodic lattices into discrete parts that can then be mass-manufactured, and when combined with a reversible connection, reconfigured and repaired to adapt to changing mission criteria. These properties can be leveraged to achieve scalable construction of architected cellular solids while utilizing high-performance materials which are not available to additive manufacturing methods, such as unidirectional carbon fiber reinforced polymer [9]. This method has been successfully demonstrated in aerospace applications, such as shape-morphing aircraft [10] and reconfigurable human-scale structures [11].

Here, this approach will be combined with recent advances in affordable, high powered laser machining technology to result in a method for assembling metallic building block elements into scalable lattice structures (FIGURE 1).

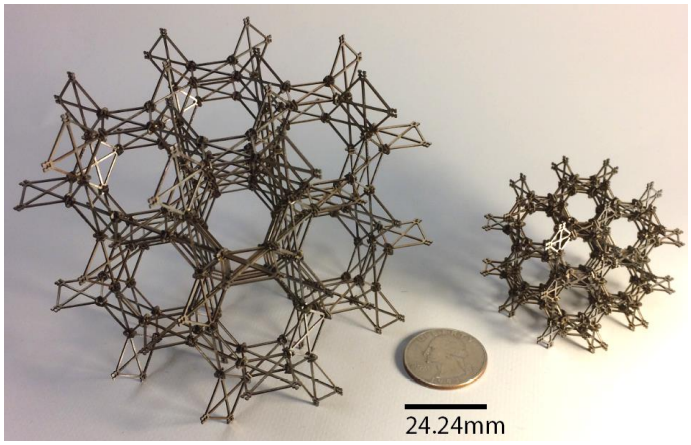

FIGURE 1: SAMPLE METALLIC LATTICE SPECIMENS BUILT USING DMLA. SEE TABLE 2 FOR PROPERTIES.

While existing commercially available AM processes such as powder bed fusion and directed energy deposition [12] have many attributes, DMLA offers unique advantages.

First, with DMLA, inert gas is not required, a support structure is not needed, the build angle constraint is removed, and parts are produced without in-built stress. Collectively, this will simplify the process of translating design intent into hardware produced and provide more design freedom. When the raw material is a metal powder or wire, the fusion process to agglomerate feedstock typically requires high temperature and an inert gas or vacuum to guarantee good final part material properties. Limitations of build angle are present and support structure is often needed [13]. Stress can also be in-built from differential heating and cooling within the parts as they build, causing part distortion [14], and parts often require a heat treatment cycle following build.

Second, the DMLA approach has the advantage of being completely recyclable. This is a unique aspect of this approach. The fine metal powder used in powder bed fusion technology requires expensive containment systems, as well as pre- and post-processing, and recycling of unused powder from a build will require extra equipment. Together with the combustion risk presented by reactive powdered metals, this approach requires significant overhead. While a wire-fed solution will remove some of the powder handling challenges once the wire has been fused into a functional part, significant energy will be required to transform the part back into wire if it is to be recycled.

Third, the DMLA approach offers the opportunity to transition rapidly between different materials; a challenge with existing commercially available metal AM processes. This approach is capable of using high performance aerospace alloys such as Ti64, Inconel, and stainless steel. In the case of the DMLA approach, the head and feedstock mechanism remains constant, no time-consuming thermal processes are present, and no support material is needed.

METHOD

Lattice Geometry

We can analytically predict the behavior of an architected cellular solid by relating its relative density to mechanical properties such as strength and stiffness. This relationship takes the form of a power law, where the ratio of macroscopic stiffness E^* and constituent material stiffness E are related to the ratio of cellular solid density ρ^* and constituent material density ρ [15]:

$$E^*/E \approx k(\rho^*/\rho_s)^a \quad (1)$$

Here, a depends on the governing microstructural behavior of the geometry of the lattice selected, and k depends on the direction of the applied load for given geometry.

We introduce a lattice geometry based on the superposition of two bending-dominated lattice geometries [2], where $a = \sim 2$, resulting in a stretch-dominated lattice geometry, where $a = \sim 1$, which we call "reinforced kelvin" (FIGURE 2). We will determine these values for the reinforced kelvin lattice geometry through experimental testing.

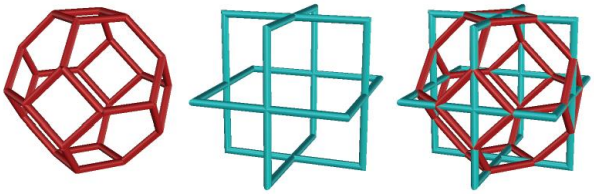

FIGURE 2: LATTICE GEOMETRY DECOMPOSITION. (L TO R) KELVIN CELL, MULTI-AXIS REINFORCEMENT CELL, RESULTING REINFORCED KELVIN CELL.

Building Block Design

We can ensure our lattice to behaves properly by designing specific areas of the structure to have failure loads relative to other areas (Figure 3-B). We will start with a strut with a square cross section with thickness t, and strut length of roughly $10t$. From here, we determine the axial compressive force resulting in buckling using Euler buckling of long slender columns:

$$F = \frac{\pi^2 EI}{(KL)^2} \quad (2)$$

where E is the elastic modulus of the material, I is the second moment of area of the strut cross section, K is an effective length multiplier based on boundary conditions, and L is strut length.

By replacing I with $t^4/12$, and L with $10t$, we can approximate $F = \sim 0.02Et^2$. Next, we can find the failure load for the joint, which consists of areas 2 and 3. Area 2 will fail in tension from a force

$$F = EA * 2 \quad (3)$$

where A is the cross-sectional area, and we multiply by 2 due to the load being shared by a pair of joint members. We can find $F = 2Et^2$, which is 100x the value of the strut failure load. Last, we want to determine the failure of the shear clips. By using the same material as the lattice elements, we calculate shear stress

$$\tau = F/2A \quad (4)$$

due to the clip being in double shear. For a metallic super alloy, the shear modulus is roughly 1/3 the elastic modulus, so we can approximate the force causing failure in shear to be $F = \sim 0.66Et^2$, which is 33x the value of the strut failure.

The joint mass does not determine the global stiffness of the architected cellular lattice, but it is included when calculating the density of the overall material, so it is desirable to reduce this "parasitic mass" as much as possible.

The current fastener design is based on a shear clip, which relies on the cross section of its members to resist tensile forces transferred from lattice part to lattice part. This is in contrast to a member axially aligned with this force, in which case the fastening method itself would be required to withstand this force (ie: a nut and bolt). Through numerous experiments it was determined that a central member with two snap-fit clips succeeded in balancing ease of installation with sufficient cross-sectional area. Lastly, it was determined empirically that two opposing clips provided a retaining force with more symmetry than a single clip alone (FIGURE 3).

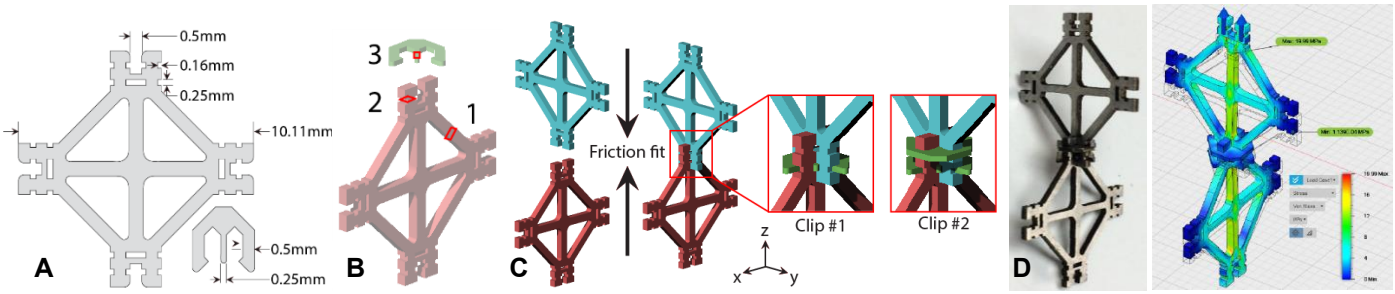

FIGURE 3: LATTICE DESIGN AND ASSEMBLY. A) LATTICE PART AND CLIP DIMENSIONS; B) CRITICAL MEMBER AREA SECTIONS FOR LATTICE BEHAVIOR (1-CLIP SHEAR, 2-JOINT SHEAR, 3-STRUT BUCKLING); C) ASSEMBLY SEQUENCE (NOTE: CLIP INSTALL DIRECTION AS SHOWN IS ALONG 45 AND 225 DEG IN XY PLANE); D) JOINT ASSEMBLY AND FEA SHOWING STRESS CONCENTRATIONS ARE HIGHER IN THE STRUTS THAN THE JOINTS.

Manufacturing and Assembly

Due to recent advances in fiber laser technology, affordable machining platforms with impressive specifications have become available. The FabLight [16] used for the work presented here is an air-cooled, pulsed 3kW laser cutter with repeatability of 0.0127mm, accuracy of ±0.167mm/meter, and a 0.1mm width kerf. This is an order of magnitude smaller than typical kerfs for abrasive waterjet cutting (0.76mm) The smallest feature on the parts are a slot with a depth of 0.16mm (FIGURE 4).

The parts are cut from 0.508mm thick 301 stainless steel sheet, with bulk material properties $E = 205\ GPa$ and $\rho = 7900\ kg/m^3$. There is slag that has to be removed, which can be done using a medium-to-coarse grit sandpaper (FIGURE 4). This can be done manually for small batches, and for larger batches an orbital sander can be used. Cut times are listed in Table 1. The parts are then manually assembled, following a process shown in FIGURE 3. Lattice elements are interconnected manually, and the clips are installed using needle-nose pliers. On average, a single pair of parts and two clips can be assembled in 1 minute. Total assembly times are listed in Table 1.

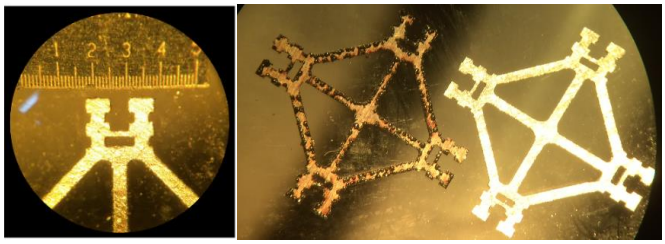

FIGURE 4: MANUFACTURING DETAILS. **(L) JOINT TIP FEATURES, SCALE SHOWN IS IN MM. (R)** BEFORE AND AFTER SLAG REMOVAL USING SAND PAPER.

TABLE I. DISCRETE METAL LATTICE ASSEMBLY (DMLA) BUILD TIME

Process/step	Time/step (sec)	Quantity	Time/process (min)
Lattice building block cutting	60	94	94
Clip cutting	5	288	24
Deburr, part removal	15	1	15
Part + clip assembly	60	~150	150
Total			283

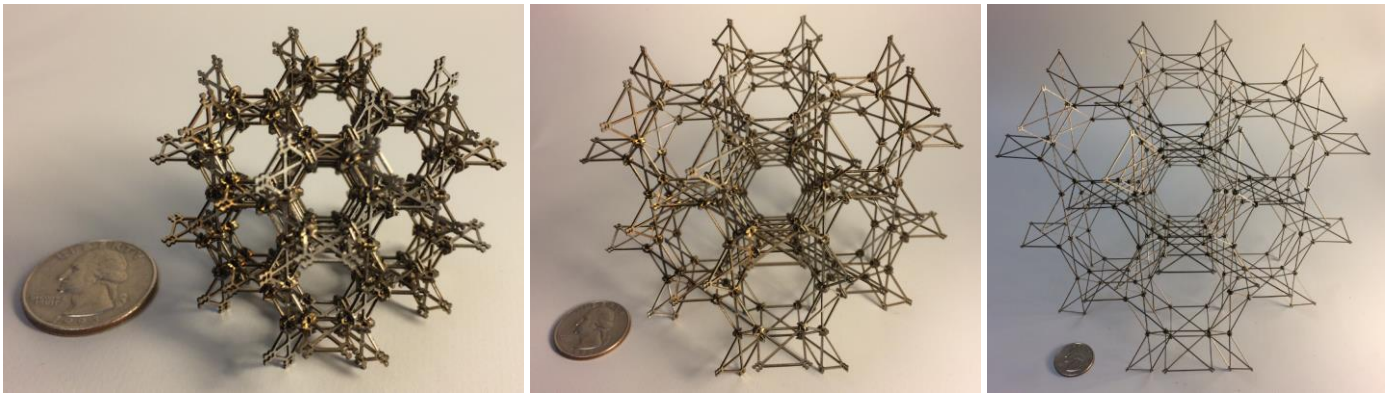

FIGURE 5: BUILT LATTICE SPECIMENS. **(L TO R) SMALL, MEDIUM, AND LARGE**, SEE TABLE 2 FOR PROPERTIES.

RESULTS

Three lattice specimens were assembled and tested, as shown in Figures 5-8. The goal was to demonstrate the manufacturing method at multiple scales, and to extract mechanical data from the built specimens.

The parts were tested in uniaxial compression using an Instron 5985 with a 5kN capacity load cell. Fixturing was designed to constrain the boundaries of the specimen in all six degrees of freedom (translation and rotation in x, y, and z). Load was applied using controlled displacement of 10mm/min up until the start of non-linear force-displacement regime, and cycled to this point five times. Then load was applied up into the non-linear regime to examine high strain deformation modes.

TABLE II. ASSEMBLED LATTICE PROPERTIES

Parameter	Small	Medium	Large
Mass	11.25g	20.35g	29.7g
Lattice strut length	5.74mm	11.48mm	22.95mm
Specimen side length	4.24cm	8.43cm	16.6cm
Volume	76.2 cm^3	599 cm^3	4574 cm^3
Volume Fraction	1.8%	0.4%	0.08%
Effective Density	151 kg/m^3	31 kg/m^3	9.14 kg/m^3
Effective Modulus	34 MPa	7.5 MPa	1 MPa
Maximum Load	2300 N	760 N	140 N
Load : mass ratio	20,000:1	3,880:1	480:1

DISCUSSION

Lattice Property Scaling

Prior art in additive manufacturing of metallic lattices shows that due to manufacturing constraints such as support structure for overhangs, only certain geometries can be achieved [17]. This "gyroid" lattice geometry has a quadratic scaling relationship between relative modulus and relative density [18]. Other geometries made with SMLS have shown near linear scaling, but this is using a lattice geometry with vertical elements oriented with the load direction, but not in any other direction, thus resulting in a lattice which is not isotropic. The scaling value for the DMLA lattice is shown to be approximately $a = 1.25$ (FIGURE 9). This is better than quadratic scaling ($b = 2$), and thus implies linear scaling [2].

Manufacturing Scaling

As noted in Langford, et al [19], a custom gantry-based machine can be designed to place discrete building block parts at a rate of 0.2 Hz (1 part per 5 seconds). However, that system does not have the same structural performance as the discrete lattice system presented here. Specifically, the joints are friction fit, and have little to no tensile capacity. Nonetheless, we can project what an automated assembly system would be able to achieve based on this prior art. We will assume 5 seconds per part placement. A full "assembly" sequence consists of the following: 1) Place lattice element (5 sec), 2) Place clips (5 sec/clip, 10 sec total). This results in a total assembly sequence time of 15 seconds per cycle, or 0.0667 Hz.

Comparing this directly to MLAM and AMD requires qualifications. For MLAM, the most time-sensitive step is the actual laser manufacturing, although there is also significant time required for pre- and post-processing [20]. Conversely, for AMD, the lattice generation and plating can be quite quick (on the order of minutes), but significant time is required for pre-plating curing, and post-plating etching removal of the base polymer lattice [21]. A summary of comparison between the methods is found in Table 3.

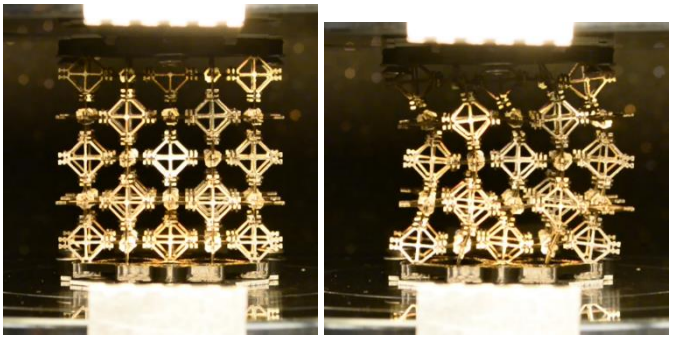

FIGURE 6: UNIDIRECTIONAL COMPRESSION TESTING OF "SMALL" DMLA SPECIMEN. SEE TABLE 2 FOR PROPERTIES

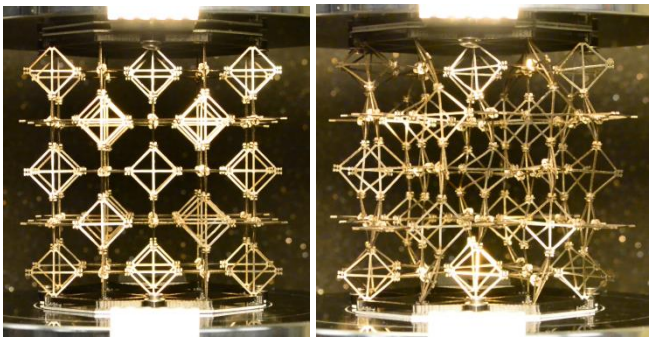

FIGURE 7: UNIDIRECTIONAL COMPRESSION TEST OF "MEDIUM" DMLA SPECIMEN. SEE TABLE 2 FOR PROPERTIES

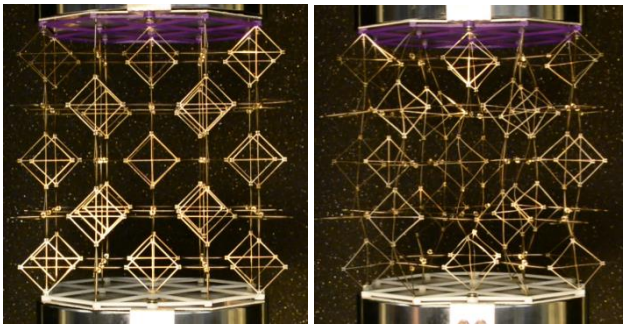

FIGURE 8: UNIDIRECTIONAL COMPRESSION TEST OF "LARGE" DMLA SPECIMEN. SEE TABLE 2 FOR PROPERTIES

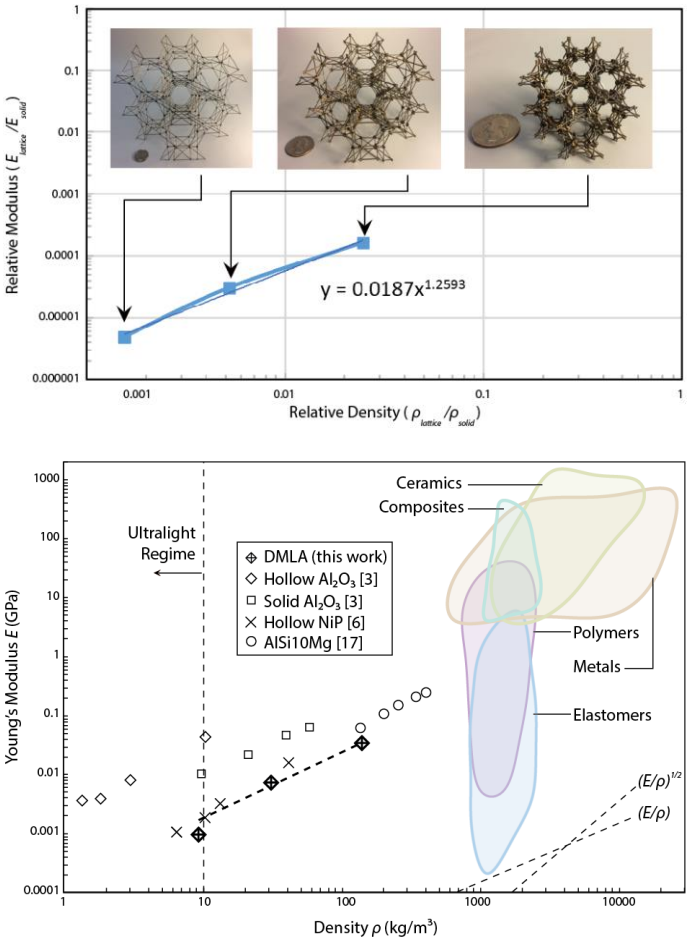

FIGURE 9: MEASUREMENT OF MATERIAL PROPERTIES OF DMLA SPECIMENS. (TOP) COMPARATIVE PLOT OF RELATIVE MODULUS V RELATIVE STIFFNESS. THE SLOPE OF THIS LINE GIVES OUR SCALING VALUE, a = 1.26. (BOTTOM) COMPARATIVE PLOT OF YOUNG'S MODULUS V DENSITY FOR METAL LATTICES AND OTHER MATERIALS.

It should be noted that this proposed gantry-based method, as depicted in FIGURE 10, suffers from the same scale limitations as the aforementioned additive manufacturing methods, specifically, that the specimen size is limited by the build envelope, and to achieve a large specimen, you need an equally large machine. Mobile robots can perform construction, such as brick-laying [22], though these require complex vision and metrology systems to maintain accuracy over long distances. To bypass this, it is possible to design robots to traverse directly upon the surface building block-based lattice structures [23], which can enable precise construction of arbitrarily large structures.

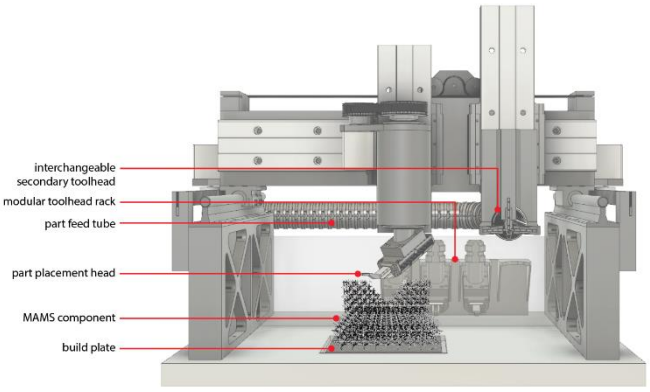

FIGURE 10: ARTIST'S CONCEPT OF AUTOMATED DISCRETE METAL LATTICE ASSEMBLY (DMLA) **PLATFORM.** IMAGE CREDIT: WILL LANGFORD, CENTER FOR BITS AND ATOMS, MIT.

In summary, the use of discrete metal lattice assembly (DMLA) has been described. The dimensional constraints and guidelines have been used to design three densities of metal lattices, made from 0.5mm thick 301 stainless steel. A newly available fiber-laser machine was used to cut sub-millimeter scale features on millimeter scale parts to build centimeter scale structures. The resulting lattices have volume fractions of 1.8%, 0.4% and 0.08%, and yielded in unidirectional compression at loads of 2300N, 760N, and 140N, respectively. The novel lattice geometry has sub-quadratic scaling which makes it appealing for applications requiring high stiffness to weight ratios. This process, when compared to other processes for manufacturing metallic lattice structures, has a number of benefits.

Existing methods can achieve either ultralight densities at small scale, or higher densities at larger scale. The former, AMD, faces challenges achieving large-scale, high throughput manufacturing. The latter, MLAM, can build at larger scales, but issues with support removal and overhangs would make ultralight densities prohibitively difficult. DMLA shows promise for combining desirable characteristics of large scale and low density for metal lattices with isotropic, sub-quadratic scaling properties.

TABLE III. COMPARISON OF METAL LATTICE MANUFACTURING METHODS

Method	Scale Range (m) (min feature – max part size)	Density Range (kg/m^3)	Build Rate (g/min)	Strength	Weakness
Additive Manufacturing and Deposition (AMD)	$10^{-8} – 10^{-2}$	$10^{0} – 10^{1}$	10^{-4} [21]	High performance + resolution	Small scale, low throughput
Discrete Metal Lattice Assembly (DMLA)	$10^{-4} – 10^{-1}$	$10^{0} – 10^{2}$	$10^{-2} – 10^{-1}$	Large dynamic range, competitive throughput	Requires automation
Metal Laser Additive Manufacturing (MLAM)	$10^{-4} – 10^{0}$	$10^{2} – 10^{3}$	10^{-1} [20]	High throughput	Geometric constraints on performance

ACKNOWLEDGEMENTS

This research was supported by NASA grants #NNX14AM40H and #NNX14AG47A, as well as Center for Bits and Atoms consortia funding.

REFERENCES

[1] M. F. Ashby, "The properties of foams and lattices.," *Philos. Trans. A. Math. Phys. Eng. Sci.*, vol. 364, no. 1838, pp. 15–30, 2006.

[2] V. S. Deshpande, M. F. Ashby, and N. a. Fleck, "Foam topology: Bending versus stretching dominated architectures," *Acta Mater.*, vol. 49, no. 6, pp. 1035–1040, 2001.

[3] X. Zheng *et al.*, "Ultralight, ultrastiff mechanical metamaterials.," *Science*, vol. 344, no. 6190, pp. 1373–7, 2014.

[4] X. Zheng and et al, "Multiscale metallic metamaterials," *Nat. Mater.*, 2016.

[5] J. Bauer, L. R. Meza, T. A. Schaedler, R. Schwaiger, X. Zheng, and L. Valdevit, "Nanolattices: An Emerging Class of Mechanical Metamaterials," *Advanced Materials*, vol. 29, no. 40. 2017.

[6] T. A. Schaedler *et al.*, "Ultralight metallic microlattices," *Science (80-.).*, vol. 334, no. 6058, pp. 962–965, 2011.

[7] H. N. G. Wadley, N. a. Fleck, and A. G. Evans, "Fabrication and structural performance of periodic cellular metal sandwich structures," *Compos. Sci. Technol.*, vol. 63, no. 16, pp. 2331–2343, 2003.

[8] H. N. G. Wadley, "Multifunctional periodic cellular metals.," *Philos. Trans. A. Math. Phys. Eng. Sci.*, vol. 364, no. 1838, pp. 31–68, 2006.

[9] K. C. Cheung and N. Gershenfeld, "Reversibly assembled cellular composite materials.," *Science*, vol. 341, no. 6151, pp. 1219–21, 2013.

[10] B. Jenett, K. C. Cheung, and S. Calisch, "Digital Morphing Wing: Active Wing Shaping Concept Using Composite Lattice-based Cellular Structures," *Soft Robot.*, vol. 3, no. 3, 2016.

[11] B. Jenett, D. Cellucci, C. Gregg, and K. C. Cheung, "Meso-scale digital materials: modular, reconfigurable, lattice-based structures," in *Proceedings of the 2016 Manufacturing Science and Engineering Conference*, 2016.

[12] W. E. Frazier, "Metal additive manufacturing: A review," *Journal of Materials Engineering and Performance*, vol. 23, no. 6. pp. 1917–1928, 2014.

[13] J. Kranz, D. Herzog, and C. Emmelmann, "Design guidelines for laser additive manufacturing of lightweight structures in TiAl6V4," *J. Laser Appl.*, vol. 27, no. S1, p. S14001, 2015.

[14] J.-P. Kruth, J. Deckers, E. Yasa, and R. Wauthle, "Assessing and comparing influencing factors of residual stresses in selective laser melting using a novel analysis method," *Proc. Inst. Mech. Eng. Part B J. Eng. Manuf.*, vol. 226, no. 6, pp. 980–991, 2012.

[15] L. Gibson, *Cellular Solids: Structure and Properties*. Cambridge University Press, 1999.

[16] "fablight." [Online]. Available: http://3dfablight.com/.

[17] C. Yan, L. Hao, A. Hussein, P. Young, and D. Raymont, "Advanced lightweight 316L stainless steel cellular lattice structures fabricated via selective laser melting," *Mater. Des.*, vol. 55, pp. 533–541, 2014.

[18] C. Yan, L. Hao, A. Hussein, S. L. Bubb, P. Young, and D. Raymont, "Evaluation of light-weight AlSi10Mg periodic cellular lattice structures fabricated via direct metal laser sintering," *J. Mater. Process. Technol.*, vol. 214, no. 4, pp. 856–864, 2014.

[19] W. Langford, A. Ghassaei, and N. Gershenfeld, "Automated Assembly of Electronic Digital Materials," in *ASME MSEC*, 2016.

[20] E. Atzeni and A. Salmi, "Economics of additive manufacturing for end-usable metal parts," *Int. J. Adv. Manuf. Technol.*, vol. 62, no. 9–12, pp. 1147–1155, 2012.

[21] A. L. Corrion, E. Clough, Z. Eckel, J. Hundley, C. Roper, and T. Schaedler, "Architected microlattice materials by self-propagating waveguide processing," in *11th Annual TechConnect World Innovation Conference and Expo, Held Jointly with the 20th Annual Nanotech Conference and Expo, and the 2017 National SBIR/STTR Conference*, 2017, vol. 1, pp. 359–362.

[22] V. Helm, S. Ercan, F. Gramazio, and M. Kohler, "Mobile robotic fabrication on construction sites: DimRob," in *IEEE International Conference on Intelligent Robots and Systems*, 2012, pp. 4335–4341.

[23] B. Jenett and K. C. Cheung, "BILL-E: Robotic Platform for Locomotion and Manipulation of Lightweight Space Structures," in *AIAA Sci-Tech*, 2017.